IEEE Access
Multidisciplinary | Rapid Review | Open Access Journal

Received August 29, 2018, accepted September 24, 2018, date of publication September 28, 2018, date of current version October 19, 2018.

Digital Object Identifier 10.1109/ACCESS.2018.2872715

Performance Analysis and Power Control of Cell-Free Massive MIMO Systems With Hardware Impairments

JIAYI ZHANG[1,2], (Member, IEEE), YINGHUA WEI[1], EMIL BJÖRNSON[3], (Senior Member, IEEE), YU HAN[2], (Student Member, IEEE), AND SHI JIN[2], (Senior Member, IEEE)

[1]School of Electronic and Information Engineering, Beijing Jiaotong University, Beijing 100044, China
[2]National Mobile Communications Research Laboratory, Southeast University, Nanjing 210096, China
[3]Department of Electrical Engineering (ISY), Linköping University, 581 83 Linköping, Sweden

Corresponding author: Jiayi Zhang (jiayizhang@bjtu.edu.cn)

This work was supported in part by the National Natural Science Foundation of China under Grant 61601020, Grant 61625106, and Grant 61725101, in part by the Beijing Natural Science Foundation under Grant 4182049 and Grant L171005, in part by the Open Research Fund of National Mobile Communications Research Laboratory, Southeast University, under Grant 2018D04, in part by the Key Laboratory of Optical Communication and Networks under Grant KLOCN2018002, in part by the National Key Research and Development Program under Grant 2016YFE0200900, in part by the Major projects of Beijing Municipal Science and Technology Commission under Grant Z181100003218010, and in part by the National Key Research and Development Program under Grant 2016YFE0200900.

ABSTRACT As an interesting network architecture for future wireless communication systems, cell-free (CF) massive multiple-input multiple-output (MIMO) distributes an excess number of access points (APs) with single or multiple antennas to cooperatively communicate with several user equipments (UEs). To realize CF massive MIMO in production, hardware impairments become a crucial problem since cheaper and low-quality antennas are needed to ensure economic and energy feasibility. In this paper, we propose a framework for performance analysis in the CF massive MIMO with classical hardware distortion models. For both uplink and downlink, closed-form spectral and energy efficiency expressions are derived, respectively. Based on these results, we provide significant insights into the practical impact of hardware impairments on CF massive MIMO. For example, the impact of hardware distortion at the APs asymptotically vanishes. Furthermore, in order to ensure uniformly good service to the users, we propose a max–min power control algorithm to maximize the minimum UE rate. Via analytical and numerical results, we prove that CF massive MIMO can tolerate hardware impairments without performance reduction.

INDEX TERMS CF massive MIMO, spectral efficiency, energy efficiency, power control, hardware impairments.

I. INTRODUCTION

To cope with the tremendous growing demand of high data rates in the fifth generation (5G) wireless networks, massive multiple-input multiple-output (MIMO) has become a essential cellular technology to achieve this requirement [2], [3]. With hundreds of antennas, massive MIMO can spatially multiplex an exclusive set of user equipments (UEs) at the same set of time-frequency resource and realize high spectral and energy efficiency. The deployment of cellular massive MIMO can be divided into two kinds of topologies. One is collocated antennas at the base station (BS), and the other is distributed antennas at the accessing points (APs).

Recently, the concept of cell-free (CF) massive MIMO has been introduced in [4]. It is a new form of network MIMO, where a large number of distributed APs equipped with single or multiple antennas serve a smaller number of distributed UEs over the coverage area. Compared to small-cell systems, CF massive MIMO yields uniformly good quality-of-service for two reasons: First, the properties of favorable propagation and channel hardening are exploited with spatially well separated UEs and multiple antennas at APs [5]; Second, a high degree of macro-diversity is achieved due to low distance between APs and UEs [6]. Further motivation, implementation concepts, and open problems in the area of CF massive MIMO can be found in [7].

Over the past three years, some initial works have studied the fundamental performance of CF massive MIMO. The spectral efficiency of CF massive MIMO has been studied in [4], which shows that a very significant gain over small-cell systems can be achieved. The work of [8] proposes a max-min

power control algorithm for CF massive MIMO to further improve the rate performance. In [6], the authors investigated the total energy efficiency considering the energy consumption of both hardware and backhaul, and proposed an optimal power allocation algorithm under a per-AP power constraint and a per-UE spectral efficiency. Using maximal-ratio combining (MRC) and zero-forcing (ZF) combining vectors, the joint power control and load balancing problem for the CF massive MIMO was investigated in [9]. In [11], the authors proposed an algorithm to assign a group of antennas to each user and solved the sum-rate maximization problem in the downlink. In [12], the authors investigated the performance of compute-and-forward in CF massive MIMO and proposed a low complexity coefficient selection algorithm. In [13], the authors proposed a user-centric approach where each AP just decoded the UE that it receives with the largest power. In [14], the authors derived an approximate per-UE downlink SE for maximum ratio transmission processing considering both uplink and downlink channel estimation errors, and power control. In [15], the authors proposed a maximum ratio transmission scheme satisfied short-term average power constraint at the APs under the effect of imperfect channel information. In [5], the authors show that we expect favorable propagation in CF massive MIMO, but not channel hardening. These works enlarge our knowledge of CF massive MIMO. However, one major limitation of the above works is that perfect transceiver hardware is assumed at APs.

The use of massive number of APs causes significant energy consumption and hardware cost due to perfect transceiver hardware components. Therefore, it is important to look into the realistic CF massive MIMO systems with non-ideal transceiver hardware components, which may induce hardware distortion. For collocated massive MIMO systems, recent works find that the impact of hardware distortion is more pronounced at the UEs than at the APs [16]–[20], [20], [21]. Note that the combination of CF massive MIMO and hardware impairments is not a straightforward extension of previous works.

Compared to our conference paper [1], which focused only on the uplink CF massive MIMO with hardware impairments, in this paper, we thoroughly investigate both uplink and downlink performance of CF massive MIMO with hardware impairments at both APs and UEs. Also, we provide a max-min power control algorithm to improve the service for all UEs. Specific contributions of the paper are summarised as follows:

- Taking into account transceiver hardware impairments, we obtain novel closed-form expressions for the spectral efficiency (SE) of uplink and downlink CF massive MIMO systems. Our results reveal that the impact of hardware impairments at both UEs and APs on the SE. These expressions are non-trivial generalization of the results for collocated massive MIMO and CF massive MIMO with perfect hardware.
- By exploring the huge degree-of-freedom offered by massive MIMO, we provide a new insightful hardware-quality scaling law to relax the constraint on hardware impairments with a large number of APs/antennas. Moreover, we derive a novel expression for uplink EE to present the optimal number of APs for different level of hardware impairments.
- Using our closed-form expressions, we propose a new max-min power control algorithm to operate the system in a fair and efficient manner. Our algorithm can improve the max-min rate as compared to heuristic schemes.

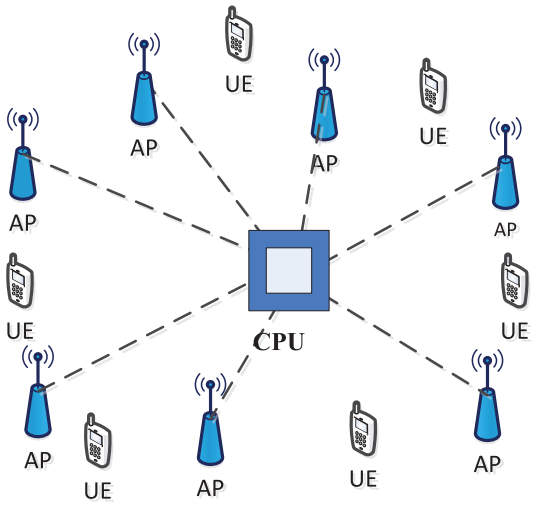

FIGURE 1. Illustration of a CF massive MIMO system.

The remainder of this paper is organized as follows. In Section II, we present the CF massive MIMO system model with hardware impairments. In Section III, we introduce the insightful expressions for the SE, scaling law, EE of uplink. In Section IV, we introduce the closed-form expressions for the SE, scaling law, EE of downlink. In Section V, we propose a max-min power control algorithm to maximize the minimum UE rates in detail. Section VI presents numerical results that validate analysis in the previous sections. Finally, some concluding remarks are made in Section VII.

NOTATION

Boldface letters are used for column vectors. The superscripts $()^*$, $()^T$, and $()^H$ stand for the conjugate, transpose, and conjugate-transpose, respectively. The Euclidean norm and the expectation operators are denoted by $\|\cdot\|$ and $\mathbb{E}\{\cdot\}$, respectively. Finally, $z \sim \mathcal{CN}\left(0, \sigma^2\right)$ denotes a circularly symmetric complex Gaussian random variable (RV) with zero mean and variance σ^2.

II. SYSTEM MODEL

As shown in Fig 1, let us consider a CF massive MIMO system distributed over a wide area and working on one time-frequency resource. There are M APs and K UEs, which are equipped with a single antenna.[1] A central processing unit (CPU) is connected with all APs with the help of

[1]Note that both APs and UEs can also be equipped with multiple antennas. Our paper implicitly supports multi-antenna APs by interpreting each antenna as a separate AP in the mathematical analysis. The extension to multi-antenna UEs is left as future work.

unlimited backhaul links. The classic flat block fading channel model [2], [4] is considered in this paper. In the uplink training of each coherent block, the APs get estimation of channel coefficients from pilot sequences transmitted simultaneously and synchronously from all UEs. These channel estimates are used for detecting the signals from the UEs and beamforming data to all UEs.

The channel response g_{mk} between AP m and UE k is assumed to be Rayleigh fading as

$$g_{mk} \sim \mathcal{CN}(0, \beta_{mk}), \quad m = 1, \ldots, M, \ k = 1, \ldots, K, \tag{1}$$

where $\beta_{mk} = \mathbb{E}\{|g_{mk}|^2\}$ is the large scale fading coefficients including path loss and shadowing effects. It is assumed that β_{mk} are known ar the CPU, since it changes slowly. In conventional co-located massive MIMO, the matrix capturing the path-loss between the base-station and the user nodes has equal diagonal elements. This is because the antennas at the base-station are co-located, and hence, the path-loss between any antenna and a particular user is the same. This property is normally used to greatly simplify the performance analysis, for example, by using results for Wishart matrices and i.i.d. random variables. However, in CF massive MIMO, the antenna elements are geographically distributed. Thus, the path-loss between any AP antenna and a user is unique. Consequence, the path-loss matrix has distinct diagonal elements, which makes the performance analysis herein substantially different and more challenging than in prior work.

A. UPLINK PILOT AND DATA TRANSMISSION

We use $q_k \sim \mathcal{CN}(0, 1)$ to denote the information symbol of the kth UE and ρ_u to denote the maximum transmit power. With the assumption of perfect transceiver hardware, the received signal sequence at the mth AP is

$$y_{um} = \sum_{k=1}^{K} g_{mk} \sqrt{\rho_u \gamma_k} q_k + w_{um}, \tag{2}$$

where $\sqrt{\gamma_k}$, $(0 \leqslant \gamma_k \leqslant 1)$ denotes the uplink power control coefficient and $w_{um} \sim \mathcal{CN}\left(0, \sigma^2\right)$ represents the additive noise. In practical CF massive MIMO systems, however, the APs and UEs may equip with low-quality hardware and suffer from hardware distortion of signals. The combine impact of different hardware distortion (such as multiplicative phase-drifts, additive distortion noise, noise amplification, and inter-carrier interference) on the system performance can be described by the tractable and well-established model from [22]. To fix the total power, the coefficient κ can reduce the signal power and it also induce an additive distortion term. Based on (2) and applying the transceiver hardware impairments model, the received signal at the mth AP is expressed as

$$y_{um} = \sum_{k=1}^{K} \sqrt{\kappa_r} g_{mk} \left(\sqrt{\rho_u \gamma_k \kappa_t} q_k + \eta_{kt} \right) + \eta_{mr} + w_{um}, \tag{3}$$

where κ_t and κ_r denote the transceiver hardware quality coefficients, respectively. The parameters $\kappa_t, \kappa_r \geqslant 0$ determine the variance of the distortion terms, where $\kappa_t = \kappa_r = 1$ represents perfect hardware and $\kappa_t = \kappa_r = 0$ represents worst-case hardware that turns all signal power into distortion. Measurements in [23] introduced that the distortion noise at the transceiver can be modeled as

$$\eta_{kt} \sim \mathcal{CN}\left(0, \left(1 - \kappa_t\right) \rho_u \gamma_k\right), \tag{4}$$

$$\eta_{mr} \left| \{g_{mk}\} \sim \mathcal{CN}\left(0, \left(1 - \kappa_r\right) \rho_u \sum_{k=1}^{K} \gamma_k |g_{mk}|^2\right). \right. \tag{5}$$

In a coherence block, the conditional distribution in (5) is given by the set of channel realizations $\{g_{mk}\}$. With the help of uplink pilot sequences, the APs estimate the channel in the uplink training phase. The pilot sequence for the kth UE is $\sqrt{\tau}\boldsymbol{\varphi}_k \in \mathbb{C}^{\tau \times 1}$, which satisfies $\left\|\boldsymbol{\varphi}_k\right\|^2 = 1$. Note that we consider arbitrary pilots in this paper. Based on (3), the received pilot signal $\mathbf{y}_{pm} \in \mathbb{C}^{\tau \times 1}$ at the mth AP is modeled as

$$\mathbf{y}_{pm} = \sum_{k=1}^{K} \sqrt{\kappa_r} g_{mk} \left(\sqrt{\tau \rho_p \kappa_t} \boldsymbol{\varphi}_k + \boldsymbol{\eta}_{kt}^p \right) + \boldsymbol{\eta}_{mr}^p + \mathbf{w}_{pm}, \tag{6}$$

where τ and ρ_p denote the pilot length and the transmit power of each pilot symbol, respectively. $\mathbf{w}_{pm} \sim \mathcal{CN}\left(\mathbf{0}, \sigma^2 \mathbf{I}_\tau\right)$ denote additive noise vector. Assuming that samples in the coherence block are independent, which can be achieved by proper pilot design, the distortion vector at the transmitter is $\boldsymbol{\eta}_{kt}^p \sim \mathcal{CN}\left(\mathbf{0}, \rho_p \left(1 - \kappa_t\right) \mathbf{I}_\tau\right)$ and the conditional distribution of the receiver distortion vector is given by

$$\boldsymbol{\eta}_{mr}^p \left| \{g_{mk}\} \sim \mathcal{CN}\left(\mathbf{0}, \rho_p \left(1 - \kappa_r\right) \sum_{k=1}^{K} |g_{mk}|^2 \mathbf{I}_\tau\right). \right. \tag{7}$$

To estimate the channel coefficient g_{mk}, the first step is to perform a despreading operation [2]. More specifically, we have $\breve{y}_{p,mk} = \boldsymbol{\varphi}_k^H \mathbf{y}_{pm}$. With the aid of linear MMSE (LMMSE) estimation, we can obtain

$$\hat{g}_{mk} = \frac{\mathbb{E}\{\breve{y}_{p,mk}^* g_{mk}\}}{\mathbb{E}\left\{\left|\breve{y}_{p,mk}\right|^2\right\}} \breve{y}_{p,mk} = c_{mk} \breve{y}_{p,mk}, \tag{8}$$

where c_{mk} is given by

$$c_{mk} \triangleq \frac{\sqrt{\tau \rho_p \kappa_r \kappa_t} \beta_{mk}}{\rho_p \sum\limits_{k'=1}^{K} \beta_{mk'} \left(\kappa_r \kappa_t \tau \left|\boldsymbol{\varphi}_k^H \boldsymbol{\varphi}_{k'}\right|^2 + \left(1 - \kappa_r \kappa_t\right) \right) + \sigma^2}. \tag{9}$$

The power of the channel estimation is given by

$$\lambda_{mk} \triangleq \mathbb{E}\left\{\left|\hat{g}_{mk}\right|^2\right\} = \sqrt{\tau \rho_p \kappa_r \kappa_t} \beta_{mk} c_{mk}. \tag{10}$$

After receiving the uplink data from the UEs, the mth AP can employ the conjugate of the LMMSE estimate $\hat{g}_{mk}$ to detect its received signal y_{um}. Through the ideal backhual links, the quantity $\hat{g}_{mk}^* y_{um}$ is sent to the CPU from each AP.

Using maximum ratio combine, the received signal at the CPU is given by

$$r_{uk} = \sum_{m=1}^{M} \hat{g}_{mk}^{*} y_{um}. \tag{11}$$

Note that other receiver combining schemes, such as ZF, could also be used. However, ZF requires exchanging the instantaneous CSI among all APs [24], which is probably infeasible in CF massive MIMO with a large number of APs.

B. DOWNLINK DATA TRANSMISSION

In the downlink data transmission, we assume that the APs treat the channel estimates as the true channels, and transmit signals to all UEs by using maximum ratio transmission. Note that there is no need for downlink pilots in multi-user MIMO systems with single-antenna UEs [22]. The transmit signal from the mth AP is given by

$$x_m = \sqrt{\rho_d \kappa_t} \sum_{k'=1}^{K} \left(\sqrt{\gamma_{mk'}} \hat{g}_{mk'}^{*} q_{k'} \right) + \eta_{mt}^{d}, \tag{12}$$

where ρ_d is the maximum transmit power of the APs, γ_{mk} is the downlink power control coefficient, and the hardware distortion of the transceiver η_{mt}^{d}, η_{kr}^{d} are given by

$$\eta_{mt}^{d} \left| \{g_{mk}\} \right. \sim \mathcal{CN}\left(0, (1-\kappa_t)\, \rho_d \sum_{k'=1}^{K} \gamma_{mk'} \left| \hat{g}_{mk'}^{*} \right|^2 \right), \tag{13}$$

$$\eta_{kr}^{d} \sim \mathcal{CN}\left(0, \rho_d^2 (1-\kappa_r) \sum_{m=1}^{M} |g_{mk}|^2 \sum_{k'=1}^{K} \gamma_{mk'} \left| \hat{g}_{mk'}^{*} \right|^2 \right). \tag{14}$$

The received signal at the kth UE from all APs is given by

$$\begin{aligned} r_{dk} &= \sqrt{\kappa_r} \sum_{m=1}^{M} g_{mk} x_m + \eta_{kr}^{d} + w_{dk} \\ &= \sqrt{\rho_d \kappa_t \kappa_r} \sum_{m=1}^{M} \sum_{k'=1}^{K} \gamma_{mk'}^{1/2} g_{mk} \hat{g}_{mk'}^{*} q_{k'} \\ &\quad + \sqrt{\kappa_r} \sum_{m=1}^{M} g_{mk} \eta_{mt}^{d} + \eta_{kr}^{d} + w_{dk}, \end{aligned} \tag{15}$$

where $w_{dk} \sim \mathcal{CN}\left(0, \sigma_d^2\right)$ is the AWGN.

III. UPLINK PERFORMANCE ANALYSIS

The uplink received signal in (11) from the data transmission can be rewritten as

$$\begin{aligned} r_{uk} = & \underbrace{\sqrt{\rho_u \gamma_k \kappa_r \kappa_t} q_k \sum_{m=1}^{M} \hat{g}_{mk}^{*} g_{mk}}_{k\text{th UE's desired signal}} + \underbrace{\sum_{m=1}^{M} \hat{g}_{mk}^{*} w_{um}}_{\text{compound noise}} \\ & + \underbrace{\sqrt{\rho_u \kappa_r \kappa_t} \sum_{m=1}^{M} \sum_{k' \neq k}^{K} \sqrt{\gamma_{k'}} q_{k'} \hat{g}_{mk}^{*} g_{mk'}}_{\text{interference between UEs}} \\ & + \underbrace{\sum_{m=1}^{M} \sum_{k'=1}^{K} \sqrt{\kappa_r} \hat{g}_{mk}^{*} g_{mk'} \eta_{k't} + \sum_{m=1}^{M} \hat{g}_{mk}^{*} \eta_{mr}}_{\text{hardware distortion}}. \end{aligned} \tag{16}$$

From the above equation, four parts are included in the received signal r_{uk}, e.g., the desired signal from the kth UE, the received noise, the interference from other UEs, and the hardware distortion from both UEs and APs. Different from prior works, we consider the non-ideal hardware components in (16), which will be used to analyse the uplink performance in the following.

A. UPLINK SPECTRAL EFFICIENCY

Let us start with the uplink SE analysis. Due to the hardware distortion, the channel estimate and estimation error are non-Gaussian distributed, which renders the standard capacity lower bound from [25] impossible. On the other hand, we use the use-and-then-forget capacity bounding technique [2] instead to derive the following result.

Theorem 1: For CF massive MIMO with hardware impairments, the uplink SE of the kth UE is given by

$$R_{uk} = \log_2 \left(1 + \frac{\kappa_r \kappa_t A_u}{\kappa_r B_u + \kappa_r C_u - \kappa_r \kappa_t A_u + (1-\kappa_r) D_u + E_u} \right), \tag{17}$$

where

$$A_u \triangleq \gamma_k \left(\sum_{m=1}^{M} \lambda_{mk} \right)^2,$$

$$B_u \triangleq \sum_{k'=1}^{K} \gamma_{k'} \left(\sum_{m=1}^{M} \lambda_{mk} \beta_{mk'} + \rho_p (1-\kappa_r) \sum_{m=1}^{M} c_{mk}^2 \beta_{mk'}^2 \right),$$

$$C_u \triangleq \sum_{k'=1}^{K} \gamma_{k'} \left(\left| \boldsymbol{\varphi}_k^H \boldsymbol{\varphi}_{k'} \right|^2 + \frac{1-\kappa_t}{\kappa_t \tau} \right) \left(\sum_{m=1}^{M} \lambda_{mk} \frac{\beta_{mk'}}{\beta_{mk}} \right)^2,$$

$$D_u \triangleq \sum_{m=1}^{M} \left(\lambda_{mk} \sum_{k'=1}^{K} \gamma_{k'} \beta_{mk'} + c_{mk}^2 (1-\kappa_r) \rho_p \beta_{mk'}^2 + c_{mk}^2 \kappa_r \rho_p \beta_{mk'} \left(\tau \kappa_t \left| \boldsymbol{\varphi}_k^H \boldsymbol{\varphi}_{k'} \right|^2 + (1-\kappa_t) \right) \right),$$

$$E_u \triangleq \frac{\sigma^2}{\rho_u} \sum_{m=1}^{M} \lambda_{mk}.$$

Proof: Please see Appendix A. ∎

Note that in Theorem 1, the uplink SE increases by deploying more APs and increasing ρ_u, which increases the SNR. The term B_u denotes the power of the non-coherent signals, while the term A_u represents the desired signal. Moreover, the term C_u is the power of the coherent signals. Due to the pilot reuse (i.e., interference from users that have non-orthogonal pilots) and the break of pilot orthogonality by the hardware impairments, the terms D_u and E_u denotes the distortion and additive noise, respectively. In Section VI, we will intuitively show that larger hardware quality terms κ_t and κ_r also improve the SE performance.

The hardware scaling law can be derived by adding more APs. More specifically, let us arbitrarily distribute the APs within a wide area, e.g., $\beta_{\min} \leqslant \beta_{mk} \leqslant \beta_{\max}$ for all m, where $0 < \beta_{\min}, \beta_{\max} < \infty$. Then, the hardware scaling law is given below.

Corollary 1: Suppose $\beta_{\min} \leqslant \beta_{mk} \leqslant \beta_{\max}$ *for all* m, *and the hardware quality factors are replaced by* $\kappa_t = \frac{\kappa_{t0}}{M^{z_t}}$, $\kappa_r = \frac{\kappa_{r0}}{M^{z_r}}$, *for some constants* $\kappa_{t0}, \kappa_{r0} > 0$, *where* z_t, z_r *is the transceiver scaling exponents. If* $z_t > 0$ *and* $z_r \geq 0$ *(or* $z_t = 0$ *and* $z_r > 1/2$*), then*

$$R_{uk} \to 0, \quad as\ M \to \infty. \tag{18}$$

If instead $z_t = 0$ *and* $0 < z_r < 1/2$, *then* $R_{uk} \to \log_2\left(1 + \mathrm{SINR}_{uk}^{\infty}\right)$ *as* M *increasing to infinity, where*

$$\mathrm{SINR}_{uk}^{\infty} = \frac{\kappa_{t0}}{\sum\limits_{k'=1}^{K} \frac{\gamma_{k'}}{\gamma_k}\left(\left|\boldsymbol{\varphi}_k^H \boldsymbol{\varphi}_{k'}\right|^2 + \frac{1-\kappa_{t0}}{\kappa_{t0}\tau}\right)\frac{\left(\sum\limits_{m=1}^{M} \mu_{mk}\frac{\beta_{mk'}}{\beta_{mk}}\right)^2}{\left(\sum\limits_{m=1}^{M} \mu_{mk}\right)^2} - \kappa_{t0}}, \tag{19}$$

and $\mu_{mk} = \frac{\rho_p \beta_{mk}^2}{\rho_p \beta_{mk} + \sigma^2}$.

Proof: All terms in (17) are divided by $\kappa_r \kappa_t A$ to obtain

$$R_{uk} = \log_2\left(1 + \frac{1}{\frac{B}{\kappa_t A} + \frac{C}{\kappa_t A} - 1 + \frac{(1-\kappa_r)D}{\kappa_r \kappa_t A} + \frac{E}{\kappa_r \kappa_t A}}\right).$$

Considering all β_{mk} are normally non-zero and limited, it is clear to see that $\frac{C}{\kappa_t A} - 1 = O\left(M^{2z_t}\right)$, which renders that $R_{uk} \to 0$ unless $z_t = 0$. We further notice that $\frac{B}{\kappa_t A} + \frac{(1-\kappa_r)D}{\kappa_r \kappa_t A} + \frac{E}{\kappa_r \kappa_t A} = O\left(M^{2z_r - 1}\right)$ when $z_t = 0$ and $z_r \geq 0$, thus these terms vanish asymptotically if $2z_r - 1 < 0$ or $z_r < 1/2$. On the other hand, if $z_r > 1/2$, all terms grow to infinity and $R_{uk} \to 0$. This proves (18).

In the case of $z_t = 0$ and $0 < z_r < 1/2$, the terms in the denominator goes to zero, except "-1" as

$$\frac{C}{\kappa_t A} \to \frac{\sum\limits_{k'=1}^{K} \gamma_{k'}\left(\left|\boldsymbol{\varphi}_k^H \boldsymbol{\varphi}_{k'}\right|^2 + \frac{1-\kappa_{0t}}{\kappa_{0t}\tau}\right)\left(\sum\limits_{m=1}^{M} \mu_{mk}\frac{\beta_{mk'}}{\beta_{mk}}\right)^2}{\kappa_{0t}\gamma_k\left(\sum\limits_{m}^{M} \mu_{mk}\right)^2}.$$

The proof concludes by derive the expression in (19). ■

It is clear to see that a trivial performance loss is suffered by using a large number of APs. However, lower hardware quality cannot be tolerated at the UEs. In practical CF massive MIMO systems, we can use low-quality APs instead of low-cost hardware at the UEs. This important result is also found in the case of cellular massive MIMO, which is quite different from the topology of CF massive MIMO.

B. UPLINK ENERGY EFFICIENCY

Now we investigate the uplink EE performance of CF massive MIMO systems with hardware impairments. It is well known that the EE (bit/Joule) is defined as the ratio of the sum rate (bit/s) to the total energy consumption (Watt) of the system. Similar to [26], a practical energy consumption model, where the total energy consumption includes the transceiver and backhaul, is employed in this paper. More specifically, the total energy consumption is given by

$$P_{\text{total}} = \sum_{k=1}^{K} P_k + \sum_{m=1}^{M} P_m + \sum_{m=1}^{M} P_{b,m}, \tag{20}$$

where P_m is the circuit power of the mth AP, $P_{b,m}$ denotes the power of the backhaul link, and P_k is the energy consumption at the kth UE. The uplink EE can be given by

$$\mathrm{EE} = \frac{\sum\limits_{k=1}^{K} R_{uk} \cdot B}{\sum\limits_{k=1}^{K} P_k + \sum\limits_{m=1}^{M} P_m + \sum\limits_{m=1}^{M} P_{b,m}}, \tag{21}$$

where B denotes the bandwidth.

IV. DOWNLINK PERFORMANCE ANALYSIS

The downlink signal (15) at the kth UE is given by

$$\begin{aligned} r_{dk} = {} & \underbrace{\sqrt{\rho_d \kappa_t \kappa_r} q_k \sum_{m=1}^{M} \gamma_{mk}^{1/2} g_{mk} \hat{g}_{mk}^{*}}_{k\text{th UE's signal}} + \underbrace{w_{dk}}_{\text{noise}} \\ & + \underbrace{\sqrt{\rho_d \kappa_t \kappa_r} \sum_{m=1}^{M} \sum_{k' \neq k}^{K} \gamma_{mk'}^{1/2} g_{mk} \hat{g}_{mk'}^{*} q_{k'}}_{\text{inter-UE interference}} \\ & + \underbrace{\sqrt{\kappa_r} \sum_{m=1}^{M} g_{mk} \eta_{mt}^{d} + \eta_{kr}^{d}}_{\text{hardware impairments}}. \end{aligned} \tag{22}$$

Note that r_{dk} also includes four parts: the desired signal from the kth UE, the inter-UE interference, the additive noise, and the hardware distortion at the UEs and APs, which makes the analysis in this paper different from prior works, which have assumed ideal hardware components. In the following, we will use (22) to investigate the downlink SE and EE.

A. DOWNLINK SPECTRAL EFFICIENCY

We use the same capacity bounding methodology as in previous work on CF massive MIMO to derive the closed-form downlink SE expression.

Theorem 2: For CF massive MIMO with hardware impairments, the downlink SE of the k*th UE is given by where*

$$A_d = \left(\sum_{m=1}^{M} \gamma_{mk}^{1/2} \lambda_{mk}\right)^2,$$

$$B_d = \sum_{m=1}^{M} \left(\lambda_{mk}\beta_{mk} + \frac{1-\kappa_t}{\kappa_t \tau}\lambda_{mk}^2 + \rho_p (1-\kappa_r) c_{mk}^2 \beta_{mk}^2\right),$$

$$\begin{aligned} C_d = {} & \sum_{k' \neq k}^{K} \left(\sum_{m=1}^{M} \gamma_{mk}\lambda_{mk'}\beta_{mk} + \rho_p (1-\kappa_r) \sum_{m=1}^{M} \gamma_{mk} c_{mk'}^2 \beta_{mk}^2 \right. \\ & \left. + \left(\sum_{m=1}^{M} \gamma_{mk}^{1/2} \lambda_{mk'} \frac{\beta_{mk}}{\beta_{mk'}}\right)^2 \left(\left|\boldsymbol{\varphi}_{k'}^H \boldsymbol{\varphi}_k\right|^2 + \frac{1-\kappa_t}{\kappa_t \tau}\right)\right), \end{aligned}$$

$$\mathrm{R}_{dk} = \log_2\left(1 + \frac{\kappa_t\kappa_r A_d}{\kappa_t\kappa_r B_d + \kappa_t\kappa_r C_d + (1-\kappa_t)\,\kappa_r D_d + (1-\kappa_r)\,E_d + \frac{1}{\rho_d}}\right), \tag{23}$$

$$D_d = \sum_{m=1}^{M} \beta_{mk}\gamma_{mk} \sum_{k'=1}^{K} \lambda_{mk'},$$

$$E_d = \rho_d \sum_{m=1}^{M} \beta_{mk} \sum_{k'=1}^{K} (\gamma_{mk'}\lambda_{mk'}).$$

Proof: Please see Appendix B. ∎

From Theorem 2, we can see that the SE increases with the number of APs. The terms B_d and C_d in the denominator represent the power of the non-coherent and coherent signals, respectively, from which the desired part A_d is subtracted. The remainder is interference and the coherent part is due to pilot contamination, caused by pilot reuse and the break of pilot orthogonality by the distortion. The terms D_d and E_d represent distortion in the transmitting AP and receiving UE, respectively. We also consider a large number of APs and have the following result.

Corollary 2: Assuming $\beta_{\min} \leqslant \beta_{mk} \leqslant \beta_{\max}$ *for all m, and the hardware quality factors are replaced by* $\kappa_t = \frac{\kappa_{t0}}{M^{z_t}}$, $\kappa_r = \frac{\kappa_{r0}}{M^{z_r}}$, *for some constants* $\kappa_{t0}, \kappa_{r0} > 0$, *where* z_t, z_r *are transceiver scaling exponents, respectively. For* $z_t > 0$ *and* $z_r \geq 0$ *(or* $z_t = 0$ *and* $z_r \geq 1$*), we have*

$$R_{dk} \to 0, \quad \text{as } M \to \infty. \tag{24}$$

If instead $z_t = 0$ *and* $0 < z_r < 1$, *then* $R_{dk} \to \log_2\left(1 + \mathrm{SIR}_{dk}^{\infty}\right)$ *as* $M \to \infty$, *where*

$$SIR_{dk}^{\infty} = \frac{\left(\sum_{m=1}^{M} \gamma_{mk}^{1/2}\lambda_{mk}\right)^2}{\sum_{k'\neq k}^{K} \gamma_{k'}\left(\sum_{m=1}^{M} \gamma_{mk}^{1/2}\lambda_{mk'}\frac{\beta_{mk}}{\beta_{mk'}}\right)^2 \left(\left|\boldsymbol{\varphi}_{k'}^H\boldsymbol{\varphi}_k\right|^2 + \frac{1-\kappa_{t0}}{\kappa_{t0}\tau}\right)}. \tag{25}$$

Proof: We first divide all terms in (23) by $\kappa_r\kappa_t A_d$ to obtain

$$\mathrm{R}_{dk} = \log_2\left(1 + \frac{1}{\frac{B_d}{A_d} + \frac{C_d}{A_d} + \frac{(1-\kappa_t)D_d}{\kappa_t A_d} + \frac{(1-\kappa_r)E_d}{\kappa_t\kappa_r A_d} + \frac{1}{\kappa_t\kappa_r\rho_d A_d}}\right). \tag{26}$$

If all β_{mk} are strictly larger than zero, it is straightforward to show that $\frac{C_d}{A_d} = O\left(M^{z_t}\right)$, which implies that $R_{dk} \to 0$ unless $z_t = 0$. We further notice that $\frac{B_d}{A_d} + \frac{(1-\kappa_t)D_d}{\kappa_t A_d} + \frac{(1-\kappa_r)E_d}{\kappa_t\kappa_r A_d} + \frac{1}{\kappa_t\kappa_r\rho_d A_d} = O\left(M^{z_r-1}\right)$ when $z_t = 0$ and $z_r \geq 0$, thus all terms asymptotically vanish if $z_r - 1 < 0$ or $z_r < 1$. In contrast, if $z_r > 1$, all terms grow to infinity and $R_{uk} \to 0$. Then (24) can be derived. ∎

Corollary 2 proves that it's tolerable to increase the hardware distortion at the APs as the number of APs increase, but not the hardware impairments at the UEs.

B. DOWNLINK ENERGY EFFICIENCY

The total downlink energy consumption can be modeled as

$$P_{total}^{d} = \sum_{m=1}^{M} P_m^d + \sum_{m=1}^{M} P_{b,m}^d, \tag{27}$$

where P_m^d denotes the circuit power at the mth AP for the downlink, $P_{b,m}^d$ is the power of the backhaul link for the mth AP. Therefore, the downlink EE is given by

$$\mathrm{EE} = \frac{\sum_{k=1}^{K} R_{dk} \cdot B}{\sum_{k=1}^{K} R_{dk} \cdot B\left(\sum_{m=1}^{M} P_m^d + \sum_{m=1}^{M} P_{b,m}^d\right)}. \tag{28}$$

V. DOWNLINK POWER CONTROL

To deliver high performance to all the UEs in the downlink regardless of their geographical locations, we propose an efficient max-min power control algorithm in this section. Since most of the traffic is in the downlink, we focus on making the downlink communication efficient. Similar power control methods might also be used in the uplink.

In the downlink, given realizations of the large-scale fading and the power constraint $\sum_{k=1}^{K} \lambda_{mk}\gamma_{mk} \leqslant 1$, we need to find the power control coefficients γ_{mk}, that maximize the minimum of the downlink rates of all users, under the power constraint $\sum_{k=1}^{K} \gamma_{mk}\lambda_{mk} \leqslant 1$. Therefore, a max-min optimization problem to optimize the above criteria can be formulated as

$$\begin{aligned} &\underset{\{\gamma_{mk}\}}{\text{maximize}} \ \min_{k=1,\ldots,K} R_{dk} \\ &\text{subject to} \ \sum_{k=1}^{K} \gamma_{mk}\lambda_{mk} \leqslant 1, \quad m = 1,\ldots,M \\ &\qquad \gamma_{mk} \geqslant 0, \quad k = 1,\ldots,K, \ m = 1,\ldots,M, \end{aligned} \tag{29}$$

where R_{dk} is given by (23). Define $\varsigma_{mk} \triangleq \gamma_{mk}^{1/2}$ and introduce the additional variables $\delta_{kk'}$, θ_k, ζ_m, ϑ_m, then (29) is equivalent to

$$\begin{aligned} &\underset{\{\varsigma_{mk},\delta_{kk'},\theta_k,\zeta_m,\vartheta_m\}}{\text{maximize}} \ \min_{k=1,\ldots,K} R_{dk} \\ &\text{subject to} \ \sum_{m=1}^{M} \varsigma_{mk'}\lambda_{mk'}\frac{\beta_{mk}}{\beta_{mk'}} \leqslant \delta_{kk'}, \quad \forall k' \neq k \\ &\qquad \sum_{m=1}^{M} \varsigma_{mk}^2\lambda_{mk}^2 \leqslant \theta_k, \quad \theta_k \geqslant 0 \\ &\qquad \sum_{k'=1}^{K} \varsigma_{mk'}^2 c_{mk'}^2 \leqslant \zeta_m, \quad \zeta_m \geqslant 0 \end{aligned}$$

$$\sum_{k'=1}^{K} \varsigma_{mk'}^2 \lambda_{mk'} \leqslant \vartheta_m, \quad 0 \leqslant \vartheta_m \leqslant 1,$$
$$m = 1, \ldots, M \quad \varsigma_{mk} \geqslant 0, \ k = 1, \ldots, K,$$
$$m = 1, \ldots, M. \tag{30}$$

Corollary 3: The function of (30) *is quasiconcave, and the program* (30) *is quasi-concave.*

Proof: Please refer to Appendix C. ■

We can resort to the bisection algorithm to solve (30) as a sequence of convex feasibility problem, as detailed in Algorithm 1.

Algorithm 1 Bisection Algorithm for Solving (30)

1) Initialization: choose the initial values of $t_{\min}$ and $t_{\max}$, where $t_{\min} = 0$ and $t_{\max} = \max\{\text{SINR}_1 \ldots \text{SINR}_K\}$ define a range of relevant values of the objective function in (30). Choose a tolerance $\varepsilon > 0$

2) Set $t = \frac{t_{\min}+t_{\max}}{2}$. Find the optimization variables $\varsigma_{mk}, k = 1, \ldots, K, m = 1, \ldots, M$ subject to:

$$\begin{cases} \|\mathbf{v}_k\| \leqslant \dfrac{1}{\sqrt{t}} \sqrt{\kappa_t \kappa_r} \displaystyle\sum_{m=1}^{M} \varsigma_{mk} \lambda_{mk}, & k = 1, \ldots, K, \\ \displaystyle\sum_{k'=1}^{K} \varsigma_{mk'}^2 c_{mk'}^2 \leqslant \zeta_m, & m = 1, \ldots, M, \\ \displaystyle\sum_{m=1}^{M} \varsigma_{mk'} \lambda_{mk'} \frac{\beta_{mk}}{\beta_{mk'}} \leqslant \delta_{kk'}, & \forall k' \neq k, \\ \displaystyle\sum_{m=1}^{M} \varsigma_{mk}^2 \lambda_{mk}^2 \leqslant \theta_k, & k = 1, \ldots, K, \\ \displaystyle\sum_{k'=1}^{K} \varsigma_{mk'}^2 \lambda_{mk'} \leqslant \vartheta_m, & m = 1, \ldots, M, \\ 0 \leqslant \vartheta_m \leqslant 1, & m = 1, \ldots, M, \\ \varsigma_{mk} \geqslant 0, & k = 1, \ldots, K, \\ & m = 1, \ldots, M, \\ \theta_k \geqslant 0, & k = 1, \ldots, K, \\ \zeta_m \geqslant 0, & m = 1, \ldots, M, \end{cases} \tag{31}$$

where $\mathbf{v}_k \triangleq \left[\mathbf{v}_{k1}^T \ \mathbf{v}_{k2}^T \ \mathbf{v}_{k3}^T \ \mathbf{v}_{k4}^T \ \frac{1}{\sqrt{\rho_d}}\right]^T$, and where

3) If the program in (31) is feasible, then set $t_{\min} = t$, else set $t_{\max} = t$.

4) Stop if $t_{\max} - t_{\min} < \varepsilon$. Otherwise, go to Step 2.

VI. NUMERICAL RESULTS

In this section, we numerically study the SE and EE of CF massive MIMO systems with hardware impairments. Within a area of size 1×1 km^2, M APs and K UEs are independently and uniformly distributed. We assume that the number of pilot sequences is equal to the number of UEs, and all UEs are assigned orthogonal pilots. The variance β_{mk} in (1) is calculated as

$$\beta_{mk} = L_{mk}^{-\alpha} \cdot 10^{\frac{z_{mk}}{10}}, \tag{32}$$

TABLE 1. Simulation Parameters for The Considered System.

Parameters	Values
noise figure	9 dB
B	20 MHz
ρ_p, ρ_u	100 mW
σ_{sh}	8 dB
α	3.5
γ_k	1

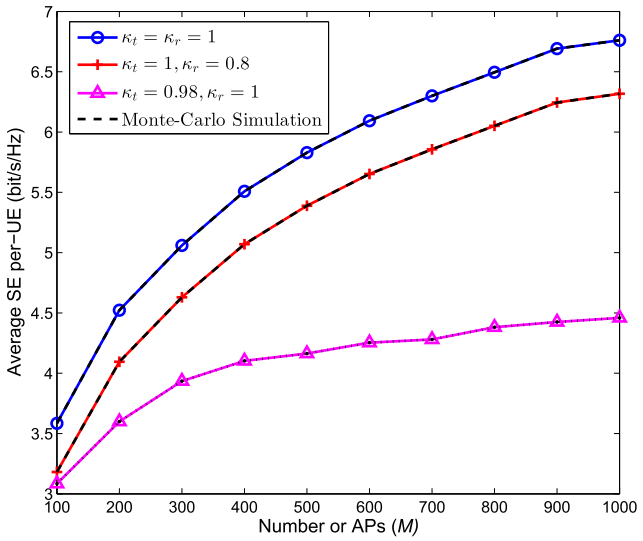

FIGURE 2. Average uplink SE per-UE as a function of the number of APs for $K = 10$. Here, $\tau = K$ and all pilot sequences are pairwise orthogonal.

where L_{mk} denotes the distance from the kth UE to the mth AP, α denotes the path loss exponent, and $z_{mk} \sim \mathcal{N}(0, \sigma_{sh}^2)$ means the shadowing effect. The key simulation parameters are summarized in Table 1. The variance of the noise is calculated as $\sigma^2 = B \cdot k_B \cdot T_0 \cdot$ noise figure (W), where $k_B = 1.381 \cdot 10^{-23}$ (Joule per Kelvin) and $T_0 = 290$ (Kelvin).

A. UPLINK

We present simulated and analytical uplink SE curves in Fig. 2, as a function of the number of APs. The Monte Carlo simulations confirm the validity of our closed-form expression. The average SE is an increasing function of M. While, the SE decreases when deploying low-quality hardware (smaller κ_t and κ_r). Nevertheless, it is clear to see that the SE is dominated by the hardware distortion at the UE (e.g., $\kappa_t = 0.98$ renders a serve impact than $\kappa_r = 0.98$).

Fig. 3 validates the hardware scaling law established by Corollary 1. Small SE loss can be found when the hardware scaling law is fulfilled ($z = 0.3$), while the curve goes asymptotically to zero when the law is not satisfied ($z = 1.1$). We also observe in Fig. 3 that the large-scale approximation converges to a non-zero limit when the hardware scaling law is fulfilled. The main difference between the three hardware scaling factor values is the convergence speed.

The CDF of the per-UE uplink SE is presented in Fig. 4 for different hardware qualities of κ_t and κ_r. We set

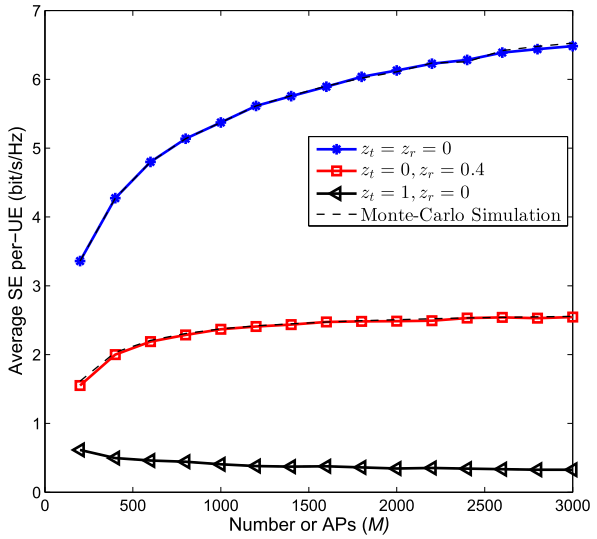

FIGURE 3. Average uplink SE per-UE against the number of APs for different hardware scaling factors z_t, z_r ($\kappa_{t0} = \kappa_{r0} = 0.0156$).

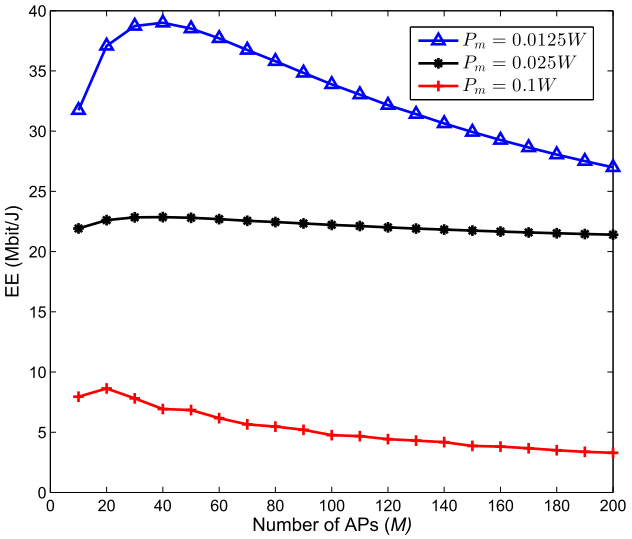

FIGURE 5. Uplink EE as a function of the number of APs for different energy consumption P_m ($K = 20$, $P_k = 0.6$ W, and $P_{b,m} = 0.1$ W).

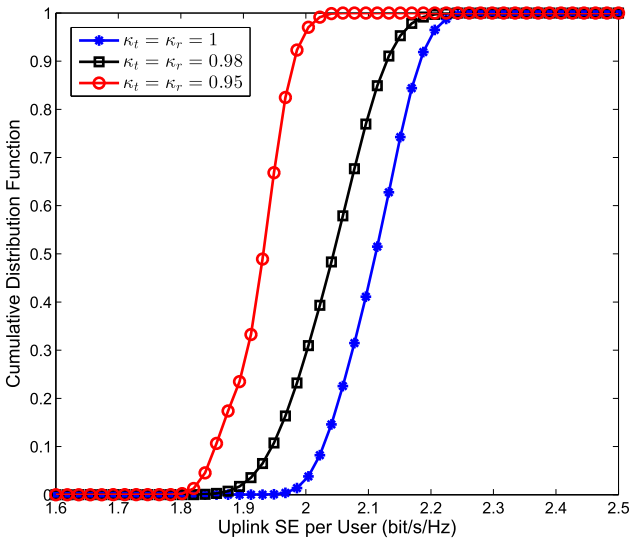

FIGURE 4. Uplink SE CDF for different levels of hardware impairments κ_t and κ_r ($M = 200, K = 60$).

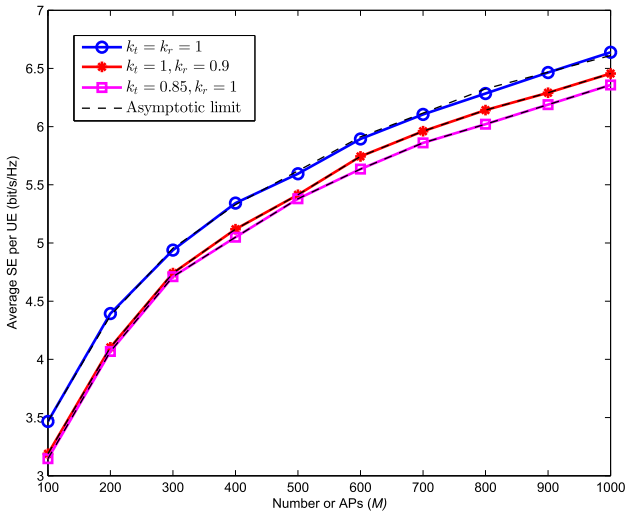

FIGURE 6. Average downlink SE per-UE as a function of the number of APs for $K = 10$. Here, $\tau = K$ and all pilot sequences are pairwise orthogonal.

$M = 200$, $K = 60$, and $\tau = 20$. It is clear that around 80% of the SE values are distributed in the range of 1.96 and 2.2 for $\kappa_t = \kappa_r = 1$, while the range is $1.89 - 2.1$ for $\kappa_t = \kappa_r = 0.98$ and $1.8 - 1.92$ for $\kappa_t = \kappa_r = 0.95$. Therefore, the uplink SE of each UE for perfect system $\kappa_t = \kappa_r = 1$ is only 5% higher than in the case when $\kappa_t = \kappa_r = 0.95$. Note that the SEs of all UEs are reduced by the hardware impairments, but the loss can be larger for the UEs that have good channels, since the distortion power is proportional to their signal power. UEs with worse channel conditions might already be limited by inter-user interference and, hence, less affected by additional distortion.

Fig. 5 shows the uplink EE in (21) against the number of APs for several values of P_m. According to [1], we assume $K = 20$, $P_k = 0.6$ W, and $P_{b,m} = 0.1$ W. It is clear that for the same number of APs, the EE reduces with the increase of P_m, which renders higher energy consumption. There exists an optimal number of M^{opt} that achieves the maximum EE. For example, $P_m = 0.0125$ W for $M^{\text{opt}} = 40$. For the case of $M \leqslant M^{\text{opt}}$, deploy more APs M can improve the EE. On the contrary, for $M > M^{\text{opt}}$, the EE rapidly decreases by increasing M. While increasing the number of APs, the SE increases to a bound while the total energy consumption still increases linearly.

B. DOWNLINK

Next, we consider the downlink, the Monte Carlo simulated and analytical average downlink SE are presented in Fig. 6,

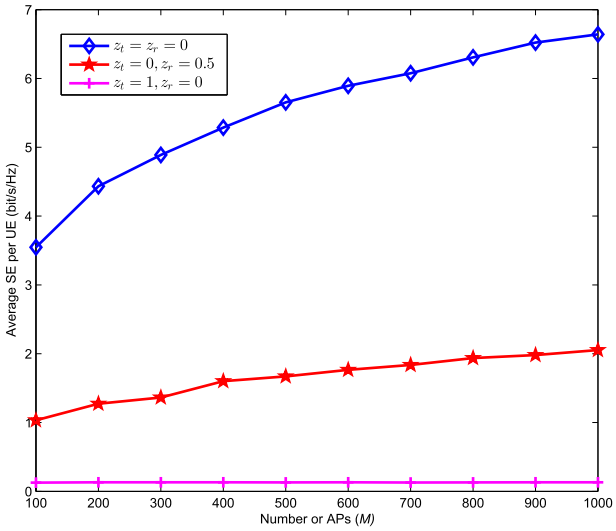

FIGURE 7. Average downlink SE per-UE against the number of APs for different hardware scaling factors z_t, z_r, ($K = 10, \kappa_{t0} = \kappa_{r0} = 0.0156$).

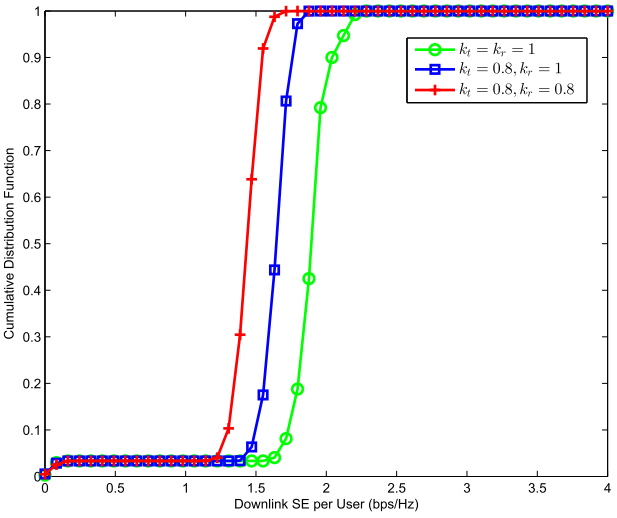

FIGURE 8. Downlink SE CDF for different levels of hardware impairments κ_t and κ_r ($M = 200, K = 60$).

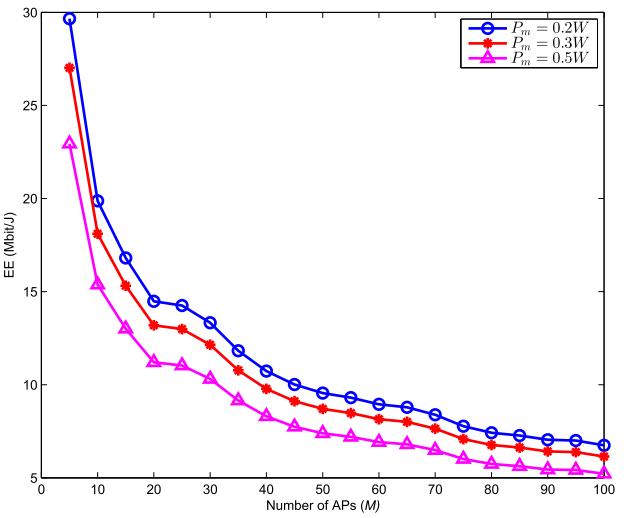

FIGURE 9. Downlink EE as a function of the number of APs for different energy consumption P_m ($K = 10$ and $P_{b,m} = 0.875$ W).

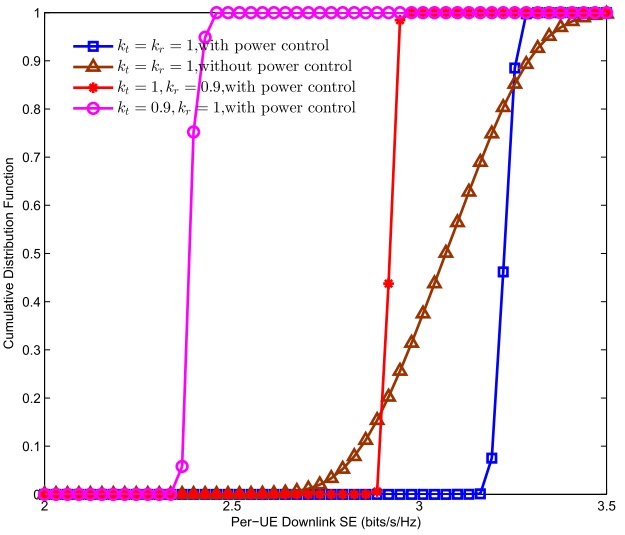

FIGURE 10. Cumulative distribution of the per-UE downlink with max-min power control (M=100, K=10).

against the number of APs. The results validate our analytical derivations. The average downlink SE is an increasing function of M, as expected. Moreover, the SE decreases when the hardware qualities κ_t and κ_r decrease.

Fig. 7 presents the downlink hardware-quality scaling law established by Corollary 2. When $z_t = z_r = 0$, the SE increases with M without bound. When $z_r = 0, 0 < z_t < 1$ (e.g., $z_r = 0.5$), the SE converges to a non-zero limit. Fig. 8 plots the CDF curves of the per-UE downlink SE for $M = 200$, $K = 60$, and $\tau = 20$, and various hardware qualities of κ_t and κ_r. It is noted that around 80% of the SE are distributed in the range of 1.8 and 2.2 for $\kappa_t = \kappa_r = 1$, while the range is $1.55 - 1.75$ for $\kappa_t = 0.8, \kappa_r = 1$ and $1.4 - 1.55$ for $\kappa_t = 0.8, \kappa_r = 0.8$. Therefore, the downlink per-UE SE for $\kappa_t = \kappa_r = 1$ is only 15% higher than in the case when $\kappa_t = 0.8, \kappa_r = 1$.

Fig. 9 studies the downlink EE in (28) against the number of APs with different P_m. In downlink, CPU take a central place to process the signals, so we assume $P_{b,m} = 0.875$ W. Compared to the uplink EE, there is a great of difference among uplink and downlink EE, since the energy consumption grows more fast, downlink EE don't have the optimal point. It is clear that the EE decreases by increasing the number of APs, due to the larger power consumption.

Fig. 10 presents the CDF of the per-UE downlink SE with max-min power control for different hardware qualities κ_t and κ_r. We find that the downlink SE range from 2.7 to 3.5 without max-min power control when $\kappa_t = \kappa_r = 1, M = 100$, $K = 10$. When taking the power control, the downlink SE range from 3.15 to 3.3 to maximize the minimum UE rate. Moreover, it is clear that the AP hardware impairments have a greater impact than the UE hardware impairments, which is also expected from our scaling law results.

VII. CONCLUSION

In this paper, we employ a well-established hardware distortion model to reveal the performance of both uplink and downlink CF massive MIMO with transceiver hardware impairments. We derive novel closed-form SE and EE expressions, which show the impact of the number and hardware quality factors of the APs and UEs on the system performance. Furthermore, a hardware scaling law is presented to prove that as the number of APs increases, the detrimental effect of hardware impairments at the APs vanishes. However, this result cannot be found for the UEs. In the following, we propose a max-min power control algorithm to maximize the smallest rate of all UEs for the downlink transmission. This algorithm greatly improves the max-min rate as compared to heuristic schemes. Our results indicate that CF massive MIMO can employ low-quality hardware at the APs to achieve considerable SE and EE performance.

APPENDIX

A. PROOF OF THEOREM 1

The received signal r_{uk} in (16) can be rewritten as

$$r_{uk} = \mathrm{DS}_k \cdot q_k + \mathrm{BU}_k \cdot q_k + \sum_{k' \neq k}^{K} \mathrm{UI}_{kk'} \cdot q_{k'} + \sum_{k'=1}^{K} \mathrm{HI}_{tkk'}^{\mathrm{UE}} + \mathrm{HI}_r^{\mathrm{AP}} + \mathrm{NI}_k, \quad (33)$$

where

$$\mathrm{DS}_k \triangleq \sqrt{\rho_u \gamma_k \kappa_r \kappa_t}\, \mathbb{E}\left\{ \sum_{m=1}^{M} \hat{g}_{mk}^* g_{mk} \right\},$$

$$\mathrm{BU}_k \triangleq \sqrt{\rho_u \gamma_k \kappa_r \kappa_t} \left(\sum_{m=1}^{M} \hat{g}_{mk}^* g_{mk} - \mathbb{E}\left\{ \sum_{m=1}^{M} \hat{g}_{mk}^* g_{mk} \right\} \right),$$

$$\mathrm{UI}_{kk'} \triangleq \sqrt{\rho_u \kappa_r \kappa_t \gamma_{k'}} \sum_{m=1}^{M} \hat{g}_{mk}^* g_{mk'},$$

$$\mathrm{HI}_{tkk'}^{\mathrm{UE}} \triangleq \sum_{m=1}^{M} \sqrt{\kappa_r}\, \hat{g}_{mk}^* g_{mk'} \eta_{k't},$$

$$\mathrm{HI}_r^{\mathrm{AP}} \triangleq \sum_{m=1}^{M} \hat{g}_{mk}^* \eta_{mr},$$

and

$$\mathrm{NI}_k \triangleq \sum_{m=1}^{M} \hat{g}_{mk}^* w_{um}.$$

By using the use-and-then-forget bounding technique [2, Chapter 3], we can obtain the SE of the kth UE as (34) at the bottom of this page. Following expectations should be computed:

$$|\mathrm{DS}_k|^2 = \rho_u \gamma_k \kappa_r \kappa_t \left(\sum_{m=1}^{M} \lambda_{mk} \right)^2, \quad (35)$$

$$\mathbb{E}\left\{ |\mathrm{BU}_k|^2 \right\} = \rho_u \gamma_k \kappa_r \kappa_t \left(\sum_{m=1}^{M} \gamma_{mk} \beta_{mk} + \frac{1-\kappa_t}{\kappa_t \tau} \left(\sum_{m=1}^{M} \lambda_{mk} \right)^2 + \rho_p (1-\kappa_r) \sum_{m=1}^{M} c_{mk}^2 \beta_{mk}^2 \right), \quad (36)$$

$$\sum_{k' \neq k}^{K} \mathbb{E}\left\{ |\mathrm{UI}_{kk'}|^2 \right\} = \rho_u \kappa_r \kappa_t \sum_{k' \neq k}^{K} \gamma_{k'} \Omega_{kk'}, \quad (37)$$

where

$$\Omega_{kk'} \triangleq \mathbb{E}\left\{ \left| \sum_{m=1}^{M} \hat{g}_{mk}^* g_{mk'} \right|^2 \right\} = \left(\sum_{m=1}^{M} \lambda_{mk} \beta_{mk'} + \left(\left| \boldsymbol{\varphi}_k^H \boldsymbol{\varphi}_{k'} \right|^2 + \frac{1-\kappa_t}{\kappa_t \tau} \right) \left(\sum_{m=1}^{M} \lambda_{mk} \frac{\beta_{mk'}}{\beta_{mk}} \right)^2 + \rho_p (1-\kappa_r) \sum_{m=1}^{M} c_{mk}^2 \beta_{mk'}^2 \right). \quad (38)$$

The above expression is used to compute

$$\sum_{k'=1}^{K} \mathbb{E}\left\{ \left| \mathrm{HI}_{tkk'}^{\mathrm{UE}} \right|^2 \right\} = \rho_u \kappa_r (1-\kappa_t) \sum_{k'=1}^{K} \gamma_{k'} \Omega_{kk'}, \quad (39)$$

$$\mathbb{E}\left\{ \left| \mathrm{HI}_r^{\mathrm{AP}} \right|^2 \right\} = (1-\kappa_r) \rho_u \sum_{m=1}^{M} \left(\lambda_{mk} \sum_{k'=1}^{K} \gamma_{k'} \beta_{mk'} + c_{mk}^2 \kappa_r \rho_p \beta_{mk'} \left(\tau \kappa_t \left| \boldsymbol{\varphi}_k^H \boldsymbol{\varphi}_{k'} \right|^2 + (1-\kappa_t) \right) + c_{mk}^2 (1-\kappa_r) \rho_p \beta_{mk'}^2 \right), \quad (40)$$

$$\mathbb{E}\left\{ |\mathrm{NI}_k|^2 \right\} = \sigma^2 \sum_{m=1}^{M} \lambda_{mk}. \quad (41)$$

The proof is completed by substituting (35)–(41) into (34).

B. PROOF OF THEOREM 2

The received signal r_{dk} in (22) can be rewritten as

$$r_{dk} = \mathrm{DS}_k^d \cdot q_k + \mathrm{BU}_k^d \cdot q_k + \sum_{k' \neq k}^{K} \mathrm{UI}_{kk'}^d \cdot q_{k'} + \mathrm{HI}_t^{\mathrm{AP}} + \mathrm{HI}_r^{\mathrm{UE}} + \mathrm{NI}_k^d,$$

$$\mathrm{R}_{uk} = \log_2 \left(1 + \frac{|\mathrm{DS}_k|^2}{\mathbb{E}\left\{ |\mathrm{BU}_k|^2 \right\} + \sum_{k' \neq k}^{K} \mathbb{E}\left\{ |\mathrm{UI}_{kk'}|^2 \right\} + \sum_{k'=1}^{K} \mathbb{E}\left\{ \left| \mathrm{HI}_{tkk'}^{\mathrm{UE}} \right|^2 \right\} + \mathbb{E}\left\{ \left| \mathrm{HI}_r^{\mathrm{AP}} \right|^2 \right\} + \mathbb{E}\left\{ |\mathrm{NI}_k|^2 \right\}} \right), \quad (34)$$

$$\mathrm{R}_{dk} = \log_2\left(1 + \frac{\left|\mathrm{DS}_k^d\right|^2}{E\left\{\left|\mathrm{BU}_k^d\right|^2\right\} + \sum_{k'\neq k}^{K} \mathrm{E}\left\{\left|\mathrm{UI}_{kk'}^d\right|^2\right\} + \sum_{k'=1}^{K} \mathrm{E}\left\{\left|\mathrm{HI}_{\mathrm{t}}^{\mathrm{AP}}\right|^2\right\} + E\left\{\left|\mathrm{HI}_{\mathrm{r}}^{\mathrm{UE}}\right|^2\right\} + E\left\{\left|\mathrm{NI}_k^d\right|^2\right\}}\right) \tag{42}$$

where

$$\mathrm{DS}_k^d \triangleq \sqrt{\rho_d \kappa_t \kappa_r}\mathbb{E}\left\{\sum_{m=1}^{M} \gamma_{mk}^{1/2} g_{mk} \hat{g}_{mk}^*\right\},$$

$$\mathrm{BU}_k^d \triangleq \sqrt{\rho_d \kappa_t \kappa_r}\left(\sum_{m=1}^{M} \gamma_{mk}^{1/2} g_{mk} \hat{g}_{mk}^* - \mathbb{E}\left\{\sum_{m=1}^{M} \gamma_{mk}^{1/2} g_{mk} \hat{g}_{mk}^*\right\}\right),$$

$$\mathrm{UI}_{kk'}^d \triangleq \sqrt{\rho_d \kappa_t \kappa_r} \sum_{m=1}^{M} \gamma_{mk'}^{1/2} g_{mk} \hat{g}_{mk'}^*,$$

$$\mathrm{HI}_t^{\mathrm{AP}} \triangleq \sqrt{\kappa_r} \sum_{m=1}^{M} g_{mk}\eta_{mt}, \mathrm{HI}_{\mathrm{r}}^{\mathrm{UE}} \triangleq \eta_{kr}, \mathrm{NI}_k^d \triangleq w_{dk}.$$

By using the use-and-then-forget bounding technique again, we can obtain the SE of the kth UE as (42) at the top of this page, where

$$\left|\mathrm{DS}_k^d\right|^2 = \rho_d \kappa_t \kappa_r \left(\sum_{m=1}^{M} \gamma_{mk}^{1/2} \lambda_{mk}\right)^2, \tag{43}$$

$$\begin{aligned}\Omega_{kk'} &= \mathbb{E}\left\{\left|\sum_{m=1}^{M} \gamma_{mk}^{1/2} g_{mk} \hat{g}_{mk'}^*\right|^2\right\} \\ &= \sum_{m=1}^{M} \gamma_{mk'}\lambda_{mk'}\beta_{mk} + \rho_p(1-\kappa_r) \\ &\quad \times \sum_{m=1}^{M} \gamma_{mk'} c_{mk'}^2 \beta_{mk}^2 \\ &\quad + \left(\sum_{m=1}^{M} \gamma_{mk'}^{1/2}\lambda_{mk'}\frac{\beta_{mk}}{\beta_{mk'}}\right)^2 \\ &\quad \times \left(\left|\boldsymbol{\varphi}_{k'}^H \boldsymbol{\varphi}_k\right|^2 + \frac{1-\kappa_t}{\kappa_t \tau}\right),\end{aligned} \tag{44}$$

$$\mathbb{E}\left\{\left|\mathrm{BU}_k^d\right|^2\right\} = \rho_d \kappa_t \kappa_r \left(\Omega_{kk} - \left(\sum_{m=1}^{M} \gamma_{mk}^{1/2}\lambda_{mk}\right)^2\right), \tag{45}$$

$$\sum_{k'\neq k}^{K} \mathbb{E}\left\{\left|\mathrm{UI}_{kk'}^d\right|^2\right\} = \rho_d \kappa_t \kappa_r \sum_{k'\neq k}^{K} \Omega_{kk'}, \tag{46}$$

$$\mathbb{E}\left\{\left|\mathrm{HI}_t^{\mathrm{AP}}\right|^2\right\} = (1-\kappa_t)\rho_d \kappa_r \sum_{m=1}^{M} \beta_{mk} \sum_{k'=1}^{K} \gamma_{mk'}\lambda_{mk'}, \tag{47}$$

$$\mathbb{E}\left\{\left|\mathrm{HI}_r^{\mathrm{UE}}\right|^2\right\} = \rho_d^2 (1-\kappa_r) \sum_{m=1}^{M} \beta_{mk} \sum_{k'=1}^{K} \gamma_{mk'}\lambda_{mk'}, \tag{48}$$

$$\mathbb{E}\left\{\left|\mathrm{NI}_k^d\right|^2\right\} = 1. \tag{49}$$

The proof is completed by substituting (43)–(49) into (42).

C. PROOF OF COROLLARY 3

Let $\mu \triangleq \{\varsigma_{mk}, \delta_{kk'}, \theta_k, \zeta_m, \vartheta_m\}$ the set of optimization variables, and we have (50), as shown at the bottom of this page. For any $t \in \mathbb{R}_+$, the upper-level set of $f(\mu)$ that belongs to μ is

$$\begin{aligned}U(f,t) &= \{\mu : f(\mu) \geqslant t\} \\ &= \left\{\mu : \|\mathbf{v}_k\| \leqslant \frac{1}{\sqrt{t}} \sum_{m=1}^{M} \varsigma_{mk}\lambda_{mk}, \forall k\right\},\end{aligned} \tag{51}$$

where $\mathbf{v}_k \triangleq \left[\mathbf{v}_{k1}^T \mathbf{I}_{-k}\ \mathbf{v}_{k2}^T\ \mathbf{v}_{k3}^T\ \mathbf{v}_{k4}^T\ \frac{1}{\sqrt{\rho_d \kappa_t \kappa_r}}\right]^T$, $\mathbf{v}_{k1} \triangleq \left[\delta_{kl}\sqrt{\left|\boldsymbol{\varphi}_{k'}^H\boldsymbol{\varphi}_k\right|^2 + \frac{1-\kappa_t}{\kappa_t\tau}}, \ldots, \delta_{kK}\sqrt{\left|\boldsymbol{\varphi}_{k'}^H\boldsymbol{\varphi}_k\right|^2 + \frac{1-\kappa_t}{\kappa_t\tau}}\right]^T$, $\mathbf{I}_{-k}$ denotes a $K \times (K-1)$ matrix which is removed the kth column from $K \times K$ identity matrix, $\mathbf{v}_{k2} \triangleq \left[\sqrt{\frac{1-\kappa_t}{\tau\kappa_t}}\theta_k^{1/2}\right]$, $\mathbf{v}_{k3} \triangleq \left[\sqrt{\rho_p(1-\kappa_r)}\beta_{1k}\zeta_1^{1/2}, \ldots, \sqrt{\rho_p(1-\kappa_r)}\beta_{Mk}\zeta_M^{1/2}\right]^T$, and $\mathbf{v}_{k4} \triangleq \left[\sqrt{\frac{\kappa_r+\rho_d(1-\kappa_r)}{\kappa_t\kappa_r}}\beta_{1k}^{1/2}\vartheta_1, \ldots, \sqrt{\frac{\kappa_r+\rho_d(1-\kappa_r)}{\kappa_t\kappa_r}}\beta_{Mk}^{1/2}\vartheta_M\right]^T$.

Since the upper-level set $U(f,t)$ is a SOC, which is a convex set. Thus, $f(\mu)$ is quasi-concave, and the constraint set in (30) is also convex. Moreover, the optimization program (30) is quasi-concave.

ACKNOWLEDGMENT

This paper was presented in part at the WCSP 2017 [1].

$$f(\mu) \triangleq \min_{k=1,\ldots,K} \frac{\left(\sum_{m=1}^{M} \varsigma_{mk}\lambda_{mk}\right)^2}{\sum_{k'\neq k}^{K} \delta_{kk'}^2\left(\left|\boldsymbol{\varphi}_{k'}^H\boldsymbol{\varphi}_k\right|^2 + \frac{1-\kappa_t}{\kappa_t\tau}\right) + \frac{(1-\kappa_t)}{\tau\kappa_t}\theta_k + \rho_p(1-\kappa_r)\sum_{m=1}^{M}\beta_{mk}^2\zeta_m + \frac{\kappa_r+\rho_d(1-\kappa_r)}{\kappa_t\kappa_r}\sum_{m=1}^{M}\beta_{mk}\vartheta_m^2 + \frac{1}{\rho_d\kappa_t\kappa_r}}. \tag{50}$$

REFERENCES

[1] J. Zhang, Y. Wei, E. Björnson, Y. Han, and X. Li, "Spectral and energy efficiency of cell-free massive MIMO systems with hardware impairments," in *Proc. Int. Conf. Wireless Commun. Signal Process. (WCSP)*, Nanjing, China, Oct. 2017, pp. 1–6.

[2] T. L. Marzetta, E. G. Larsson, H. Yang, and H. Q. Ngo, *Fundamentals of Massive MIMO*. Cambridge, U.K.: Cambridge Univ. Press, 2016.

[3] J. Zhang, L. Dai, X. Li, Y. Liu, and L. Hanzo, "On low-resolution ADCs in practical 5G millimeter-wave massive MIMO systems," *IEEE Commun. Mag.*, vol. 56, no. 7, pp. 205–211, Jul. 2018.

[4] H. Q. Ngo, A. Ashikhmin, H. Yang, E. G. Larsson, and T. L. Marzetta, "Cell-free massive MIMO versus small cells," *IEEE Trans. Wireless Commun.*, vol. 16, no. 3, pp. 1834–1850, Mar. 2017.

[5] Z. Chen and E. Björnson, "Channel hardening and favorable propagation in cell-free massive MIMO with stochastic geometry," *IEEE Trans. Wireless Commun.*, to be published.

[6] H. Q. Ngo, L. N. Tran, T. Q. Duong, M. Matthaiou, and E. G. Larsson, "Energy efficiency optimization for cell-free massive MIMO," in *Proc. IEEE Int. Workshop Signal. Process. Adv. Wireless Commun. (SPAWC)*, Sapporo, Japan, Jul. 2017, pp. 1–5.

[7] G. Interdonato, E. Björnson, H. Q. Ngo, P. Frenger, and E. G. Larsson. (Apr. 2018). "Ubiquitous cell-free massive MIMO communications." [Online]. Available: https://arxiv.org/abs/1804.03421

[8] E. Nayebi, A. Ashikhmin, T. L. Marzetta, H. Yang, and B. D. Rao, "Precoding and power optimization in cell-free massive MIMO systems," *IEEE Trans. Wireless Commun.*, vol. 16, no. 7, pp. 4445–4459, Jul. 2017.

[9] T. H. Nguyen, T. K. Nguyen, H. D. Han, and V. D. Nguyen, "Optimal power control and load balancing for uplink cell-free multi-user massive MIMO," *IEEE Access*, vol. 6, pp. 14462–14473, 2018.

[10] E. Nayebi, A. Ashikhmin, T. L. Marzetta, and B. D. Rao, "Performance of cell-free massive MIMO systems with MMSE and LSFD receivers," in *Proc. IEEE 50th Asilomar Conf. Signals, Syst. Comput.*, Nov. 2016, pp. 203–207.

[11] M. N. Boroujerdi, A. Abbasfar, and M. Ghanbari, "Antenna assignment in cell free massive MIMO systems," in *Proc. Iranian Conf. Elect. Eng. (ICEE)*, Hong Kong, May 2017, pp. 1747–1751.

[12] Q. Huang and A. Burr, "Compute-and-forward in cell-free massive MIMO: Great performance with low Backhaul load," in *Proc. IEEE Int. Conf. Commun. (ICC)*, Paris, France, May 2017, pp. 601–606.

[13] S. Buzzi and A. Zappone, "Downlink power control in user-centric and cell-free massive MIMO wireless networks," in *Proc. IEEE Int. Symp. Personal, Indoor Mobile Radio Commun. (PIMRC)*, Montreal, QC, Canada, Oct. 2017, pp. 1–6.

[14] G. Interdonato, H. Q. Ngo, E. G. Larsson, and P. Frenger, "How much do downlink pilots improve cell-free massive MIMO?" in *Proc. IEEE GLOBECOM*, Washington, DC, USA, Dec. 2016, pp. 1–7.

[15] G. Interdonato, H. Q. Ngo, E. G. Larsson, and P. Frenger, "On the performance of cell-free massive MIMO with short-term power constraints," in *Proc. IEEE Int. Workshop Comput. Aided Modeling Design Commun. Links Netw. (CAMAD)*, Lund, Sweden, Oct. 2016, pp. 225–230.

[16] E. Björnson, M. Matthaiou, and M. Debbah, "Massive MIMO with non-ideal arbitrary arrays: Hardware scaling laws and circuit-aware design," *IEEE Trans. Wireless Commun.*, vol. 14, no. 8, pp. 4353–4368, Aug. 2015.

[17] Z. Zhang, Z. Chen, M. Shen, and B. Xia, "Spectral and energy efficiency of multipair two-way full-duplex relay systems with massive MIMO," *IEEE J. Sel. Areas Commun.*, vol. 34, no. 4, pp. 848–863, Apr. 2016.

[18] J. Zhang, L. Dai, Z. He, S. Jin, and X. Li, "Performance analysis of mixed-ADC massive MIMO systems over Rician fading channels," *IEEE J. Sel. Areas Commun.*, vol. 35, no. 6, pp. 1327–1338, Jun. 2017.

[19] J. Zhang, L. Dai, S. Sun, and Z. Wang, "On the spectral efficiency of massive MIMO systems with low-resolution ADCs," *IEEE Commun. Lett.*, vol. 20, no. 5, pp. 842–845, Feb. 2016.

[20] J. Zhang, L. Dai, X. Zhang, E. Björnson, and Z. Wang, "Achievable rate of Rician large-scale MIMO channels with transceiver hardware impairments," *IEEE Trans. Veh. Technol.*, vol. 65, no. 10, pp. 8800–8806, Oct. 2016.

[21] E. Björnson, J. Hoydis, M. Kountouris, and M. Debbah, "Massive MIMO systems with non-ideal hardware: Energy efficiency, estimation, and capacity limits," *IEEE Trans. Inf. Theory*, vol. 60, no. 11, pp. 7112–7139, Nov. 2014.

[22] E. Björnson, J. Hoydis, and L. Sanguinetti, "Massive MIMO networks: Spectral, energy, and hardware efficiency," *Found. Trends Signal Process.*, vol. 11, nos. 3–4, pp. 154–655, 2017.

[23] C. Studer, M. Wenk, and A. Burg, "MIMO transmission with residual transmit-RF impairments," in *Proc. ITG/IEEE Works. Smart Antennas*, Feb. 2010, pp. 189–196.

[24] L. D. Nguyen, T. Q. Duong, H. Q. Ngo, and K. Tourki, "Energy efficiency in cell-free massive MIMO with zero-forcing precoding design," *IEEE Commun. Lett.*, vol. 21, no. 8, pp. 1871–1874, Aug. 2017.

[25] J. Hoydis, S. ten Brink, and M. Debbah, "Massive MIMO in the UL/DL of cellular networks: How many antennas do we need?" *IEEE J. Sel. Areas Commun.*, vol. 31, no. 2, pp. 160–171, Feb. 2013.

[26] H. Q. Ngo, L.-N. Tran, T. Q. Duong, M. Matthaiou, and E. G. Larsson, "On the total energy efficiency of cell-free massive MIMO," *IEEE Trans. Green Commun. Netw.*, vol. 2, no. 1, pp. 25–39, Mar. 2018.

JIAYI ZHANG (S'08–M'14) received the B.Sc. and Ph.D. degrees in communication engineering from Beijing Jiaotong University, China, in 2007 and 2014, respectively. Since 2016, he has been a Professor with the School of Electronic and Information Engineering, Beijing Jiaotong University, China. From 2014 to 2016, he was a Post-Doctoral Research Associate with the Department of Electronic Engineering, Tsinghua University, China. From 2014 to 2015, he was also a Humboldt Research Fellow with the Institute for Digital Communications, University of Erlangen-Nuermberg, Germany. From 2012 to 2013, he was a Visiting Ph.D. Student with the Wireless Group, University of Southampton, U.K. His current research interests include massive MIMO, unmanned aerial vehicle systems, and performance analysis of generalized fading channels.

He was recognized as an Exemplary Reviewer of the IEEE Communications Letters in 2015 and 2016. He was also recognized as an Exemplary Reviewer of the IEEE Transactions on Communications in 2017. He serves as an Associate Editor for the IEEE Communications Letters and IEEE Access.

YINGHUA WEI is currently pursuing the master's degree in electronic engineering from Beijing Jiaotong University, Beijing, China. Her research interests include massive MIMO systems, and signal processing for wireless communications.

EMIL BJÖRNSON (S'07–M'12–SM'17) received the M.S. degree in engineering mathematics from Lund University, Sweden, in 2007, and the Ph.D. degree in telecommunications from the KTH Royal Institute of Technology, Sweden, in 2011. From 2012 to 2014, he held a joint post-doctoral position at the Alcatel-Lucent Chair on Flexible Radio, Supelec, France, and KTH. He joined Linköping University, Sweden, in 2014, where he is currently an Associate Professor and a Docent with the Division of Communication Systems.

He performs research on multi-antenna communications, massive MIMO, radio resource allocation, energy-efficient communications, and network design. He is the first author of the textbooks *Massive MIMO Networks: Spectral, Energy, and Hardware Efficiency* (2017) and *Optimal Resource Allocation in Coordinated Multi-Cell Systems* (2013). He is dedicated to reproducible research and has made a large amount of simulation code publicly available. He has been on the Editorial Board of the IEEE Transactions on Communications since 2017 and the IEEE Transactions on Green Communications and Networking since 2016.

He has performed MIMO research for over 10 years and has filed over 10 related patent applications. He received the 2018 Marconi Prize Paper Award in Wireless Communications, the 2016 Best Ph.D. Award from EURASIP, the 2015 Ingvar Carlsson Award, and the 2014 Outstanding Young Researcher Award from the IEEE ComSoc EMEA. He also co-authored papers that received best paper awards at the conferences the IEEE ICC 2015, WCSP 2017, IEEE WCNC 2014, IEEE SAM 2014, IEEE CAMSAP 2011, and WCSP 2009.

YU HAN (S'14) received the B.S. degree in communications engineering from Hangzhou Dianzi University, Hangzhou, China, in 2012, and the M.S. degree in communications and information systems from Southeast University, Nanjing, China, in 2015, where she is currently pursuing the Ph.D. degree in information and communications engineering. Her research interests include massive multiple input multiple output, millimeter wave, multiuser transmission schemes, and beamforming techniques.

SHI JIN (S'06–M'07) received the B.S. degree in communications engineering from the Guilin University of Electronic Technology, Guilin, China, in 1996, the M.S. degree from the Nanjing University of Posts and Telecommunications, Nanjing, China, in 2003, and the Ph.D. degree in communications and information systems from Southeast University, Nanjing, in 2007. From 2007 to 2009, he was a Research Fellow with the Adastral Park Research Campus, University College London, London, U.K. He is currently with the faculty of the National Mobile Communications Research Laboratory, Southeast University. His research interests include space time wireless communications, random matrix theory, and information theory. He serves as an Associate Editor for the IEEE TRANSACTIONS ON WIRELESS COMMUNICATIONS, and the IEEE COMMUNICATIONS LETTERS, and *IET Communications*. He and his co-authors have received the 2011 IEEE Communications Society Stephen O. Rice Prize Paper Award in the field of communication theory and the 2010 Young Author Best Paper Award from the IEEE Signal Processing Society.